

Article

Mineralogical Characteristics Study of Calcite from the Fujian Province, China

Zhe-Yi Zhao ^{1,2,3}, Yu-Tao Lin ⁴, Yi Zhao ^{2,5,*} and Bo Xu ^{1,2,3,*}¹ School of Gemology, China University of Geosciences Beijing, 29 Xueyuan Road, Haidian District, Beijing 100083, China² State Key Laboratory of Geological Processes and Mineral Resources, China University of Geosciences, Beijing 100083, China³ The Beijing SHRIMP Center, Chinese Academy of Geological Sciences, Beijing 100037, China⁴ School of Earth Sciences and Engineering, Nanjing University, 163 Xianlin Avenue, Nanjing 210023, China⁵ School of Earth Sciences and Resources, China University of Geosciences Beijing, 29 Xueyuan Road, Haidian District, Beijing 100083, China

* Correspondence: zhaoyi0102@cugb.edu.cn (Y.Z.); bo.xu@cugb.edu.cn (B.X.)

Abstract: With mineral in situ testing technology and ore deposit geochemistry development, calcite has become a hot topic in studying carbonate minerals. Four large-grain calcite crystals from Fujian, China, were used for a detailed study. This study provides a comprehensive data set through mineralogical standard properties and spectral characteristics, including Fourier transform infrared, X-ray fluorescence spectrum, and Raman spectroscopy. Major elements were analyzed using X-ray fluorescence (XRF) and Micro-XRF. A high-resolution gas-source stable isotope ratio mass spectrometer was used to test C-O isotope characteristics. The four samples' spectral characteristics and phase composition show excellent uniformity, all with the same characteristic peaks, indicating that they are pure calcite without other impurity minerals. C-O isotope characteristics indicate that Fujian calcite has mantle genetic characteristics, which may be affected by marine carbonate dissolution or sedimentary rock contamination. The variation of Fe and Mn contents may indicate that the four samples formed at different metallogenic stages.

Keywords: calcite; spectral; major elements; genesis; Fujian



Citation: Zhao, Z.-Y.; Lin, Y.-T.; Zhao, Y.; Xu, B. Mineralogical Characteristics Study of Calcite from the Fujian Province, China. *Crystals* **2023**, *13*, 51. <https://doi.org/10.3390/cryst13010051>

Academic Editor: Francesco Capitelli

Received: 21 November 2022

Revised: 20 December 2022

Accepted: 21 December 2022

Published: 27 December 2022



Copyright: © 2022 by the authors. Licensee MDPI, Basel, Switzerland. This article is an open access article distributed under the terms and conditions of the Creative Commons Attribution (CC BY) license (<https://creativecommons.org/licenses/by/4.0/>).

1. Introduction

Calcite (CaCO_3) is a common carbonate mineral found in various geological settings. The $[\text{CO}_3]$ coordination triangle is the basic structural unit of calcite, which is usually composed of $[\text{CO}_3]^{2-}$ in isolated island forms combined with Ca and often contains isomorphous components such as Mg, Fe, Mn, and rare earth elements (REE). Therefore, the geochemical characteristics of hydrothermal calcite can indicate the geochemical characteristics of the ore-forming fluid, providing important information such as the genesis of the deposit and the source of metallogenic materials [1,2].

Currently, calcite research focuses primarily on two areas: isotope and trace element geochemistry and fluid inclusion. Hou et al. studied the Sr-Nd and fluid inclusion C-O isotopes of calcite in the Mianning-Dechang REE ore belt. They proposed the metallogenic belt's source area enrichment process and fluid evolution mechanism [3,4]. On the other hand, Tang et al. investigated the trace elements and C-O isotope of calcite in the Huachangshan Pb-Zn deposit, the composition of the ore-forming fluid, and the provenance of metallogenic materials [5]. Furthermore, the analysis of fluid inclusions in calcite can also be used to determine the ore-forming conditions and mineralisation time [6].

In recent years, previous researchers have conducted detailed research on calcite in numerous deposits worldwide. These include the Oka mining area in Canada [7]; the Xikuangshan antimony deposit in central Hunan, China [8]; the Egongtang uranium

deposit in northern Guangdong, China [9]; the Nibao gold deposit in southwest China [10]; and the Singu-Tabeikkyin gold deposit in Myanmar [11]; among many others.

In this study, the mineralogical characteristics of four calcite single crystals collected from Fujian, China, were studied through spectral analysis, major element composition analysis, and isotope analysis. Spectral features are obtained and compared with the standard spectra in the RRUFF database [12]. The objective is to report the systematic mineralogical characteristics of the calcite from Fujian, China, a new production area and to discuss its possible genesis.

2. Geological Setting

The Fujian mining area is located east of the South China fold system, formed after the Early Jurassic and is adjacent to the Pacific continental arc active belt. It has a complex geological history. This area primarily extends in the N-E direction, forming three tectonic units.

The four samples in this study were produced in hydrothermal reformed deposits in the southwestern Fujian depression. The size and shape of the ore body are fault structure controlled. The calcite produced in this deposit is mostly of high crystallisation degree and the composition has a high concordant degree.

3. Materials and Methods

Four calcite crystals (FJ-1, FJ-2, FJ-3, and FJ-4) in Fujian, China, were examined using standard gemological techniques. A hydrostatic weighing method was used to determine the samples' specific gravity (SG). The samples' spectral properties and major element properties were determined using spectroscopy and X-ray fluorescence spectroscopy (XRF) tests at the Gemological Research Laboratory of China University of Geosciences (Beijing).

Infrared reflection spectroscopy was obtained using the Tensor 27 Fourier transform infrared spectrometer, with a test spectral range of 2000–400 cm^{-1} . A Raman spectroscopy test was performed using a Horiba HR Evolution-type micro-confocal laser Raman spectrometer (Horiba, Ltd., Kyoto, Japan) with the following settings: laser source: 532 nm; slit width: 100 μm ; grating: 600 gr/mm; scan time: 1s; integration times: 1; and test range: 1500–100 cm^{-1} .

The X-ray fluorescence (XRF) test is completed by an EDX-7000 energy dispersive X-ray fluorescence spectrometer in a vacuum environment. The X-ray powder diffraction (XRD) data were obtained using the Smart Lab (9KW) X-ray powder diffraction instrument (Nikoka Electric Co., Ltd., Japan) with a scanning range of $2\theta = 3\text{--}90^\circ$. The Micro-XRF test was completed in the National Infrastructure of Mineral Rock and Fossil Resources laboratory using the M4 Tomado Plus micro area X-ray fluorescence spectrometer. The element analysis range is C-Am. The C-O isotope test was completed using the Delta V Plus with GasBench high-resolution gas stable isotope mass spectrometer at Tianjin University. The details can be found in references [13–15].

4. Results

4.1. Visual Appearance and Mineralogical Properties

The Fujian calcite samples are colourless (Figure 1A,B) or yellow-brown (Figure 1C,D), with rhombic regular cleavage blocks and transparent and glassy lustre. The magnification observation of four samples reveals a double image phenomenon caused by high birefringence and two sets of surface cleavage. No significant internal inclusions have been observed. FJ-1, FJ-2, FJ-3, and FJ-4 have SG values of 2.72, 2.72, 2.69, and 2.72, respectively, and refractive index values of 1.52, 1.53, 1.51, and 1.52. The calcite samples showed no reaction when viewed through the Chelsea colour filter.

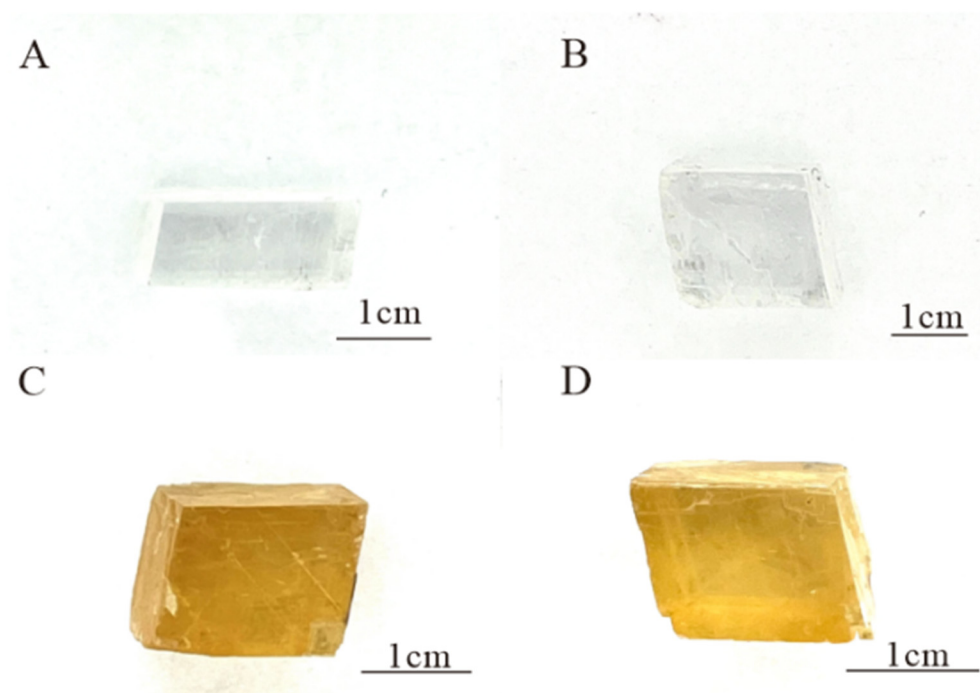


Figure 1. The calcite crystals FJ-1 (A), FJ-2 (B), FJ-3 (C), and FJ-4 (D).

4.2. Spectral Characteristics

4.2.1. Fourier Transform Infrared Spectrum

The four calcite samples have characteristic absorption peaks in the fingerprint region of 709 cm^{-1} , 887 cm^{-1} , and 1480 cm^{-1} (Figure 2). The position of 1480 cm^{-1} belongs to the internal stretching vibration of $[\text{CO}_3]^{2-}$, the position of 709 cm^{-1} belongs to the in-plane bending vibration of $[\text{CO}_3]^{2-}$, and the position of 887 cm^{-1} belongs to the out-of-plane bending vibration of $[\text{CO}_3]^{2-}$ [16,17]. Compared with RRUFF standard data, the four samples are all pure calcite with a high degree of concordance.

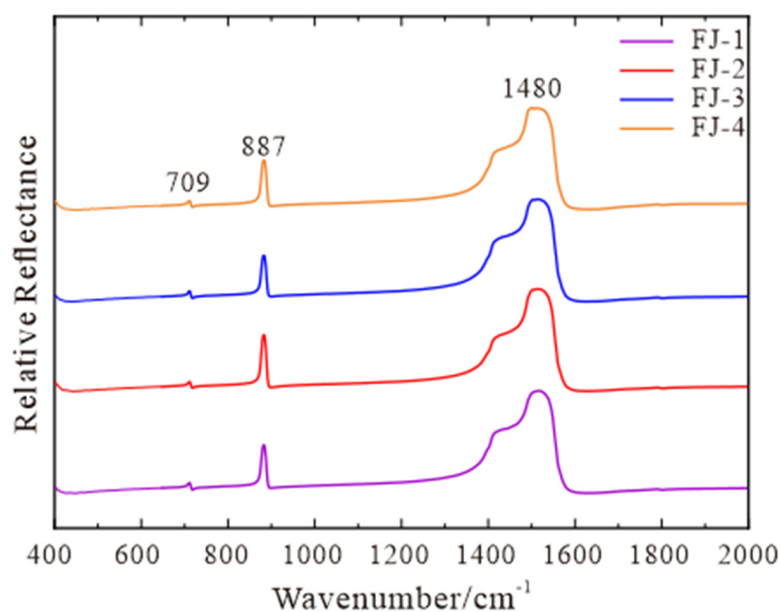


Figure 2. Fourier Transform Infrared Spectrum of FJ-1, FJ-2, FJ-3, and FJ-4.

4.2.2. Raman Spectrum

The following characteristic peaks are found within the range of 100–1500 cm^{-1} (Figure 3): an absorption peak at 713 cm^{-1} caused by the in-plane bending vibration of $[\text{CO}_3]^{2-}$, an absorption peak at 1087 cm^{-1} caused by the symmetric stretching vibration of C-O in $[\text{CO}_3]^{2-}$ group, and an absorption peak at 155 cm^{-1} and 282 cm^{-1} caused by the lattice vibration between Ca^{2+} and $[\text{CO}_3]^{2-}$ [18]. Compared with RRUFF standard data, the four samples are all pure calcite with a high degree of concordance.

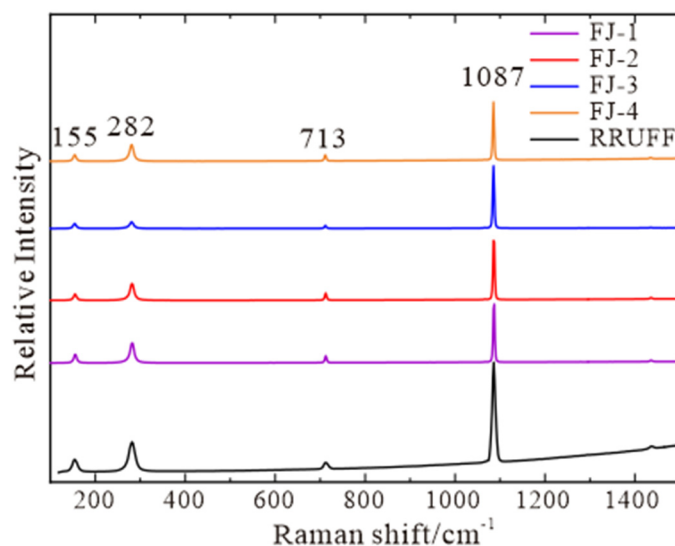


Figure 3. Raman spectra of FJ-1, FJ-2, FJ-3, and FJ-4, RRUFF standard spectra are listed for comparison.

4.3. Phase Composition

The diffraction patterns of four samples obtained by XRD experiments are shown in Figure 4 and the corresponding values for unit cell parameters are listed in Table 1.

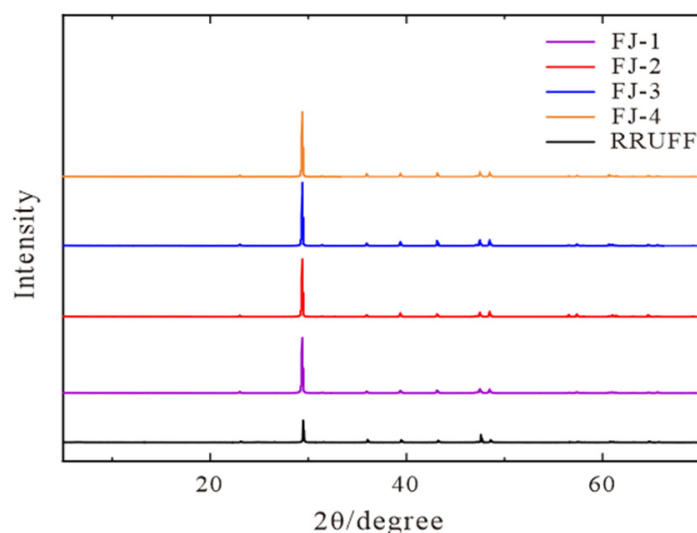


Figure 4. XRD diffraction patterns of FJ-1, FJ-2, FJ-3, and FJ-4, RRUFF standard pattern are listed for comparison.

Table 1. Unit cell parameter values of four Fujian calcite samples and RRUFF standard data are listed for comparison.

	a/Å	b/Å	c/Å	$\alpha/^\circ$	$\beta/^\circ$	$\gamma/^\circ$
FJ-1	4.987	4.987	17.053	90.0	90.0	120.0
FJ-2	4.988	4.988	17.055	90.0	90.0	120.0
FJ-3	4.987	4.987	17.055	90.0	90.0	120.0
FJ-4	4.986	4.986	17.050	90.0	90.0	120.0
RRUFF	4.987	4.987	17.050	90.0	90.0	120.0

The following seven characteristic peaks are found within the range of 10–60° (Figure 4): the strongest diffraction peak at 29.3° and the two stronger diffraction peaks at 48.5° and 47.5° correspond to the three faces of (104) (018) (116), respectively. Another four distinct diffraction peaks of 22.7°, 35.9°, 39.3°, and 43.1° correspond to the four faces of (012) (110) (113) (202). The four samples have a high degree of concordance compared to RRUFF standard data. In combination with the minimal difference (± 0.001 – ± 0.005) between the unit cell parameter values of the four samples in Table 1 and the RRUFF standard data, it is possible to prove that the phase composition of the four samples is pure calcite, without other impurity minerals. A small range of isomorphic substitution could explain the slight change in unit cell parameters.

4.4. Major Elements Characteristics

4.4.1. X-ray Fluorescence Spectrum (XRF)

XRF was used to analyse the major element composition of four samples. The results of 20 test points from four samples are nearly identical. The analysis results are presented in Table A1. It can be seen that the main component of the four samples is CaO. In addition, there is a certain amount of MnO, Fe₂O₃, SiO₂, and other elements. Ca is the most abundant, accounting for more than 90% of the total, and corresponding to the calcite's main component, CaCO₃. Si, Mn, Fe, K, Sr, and other elements were also discovered. Si has the highest concentration, reaching about 0.6–0.7%; Sr and K about 0.05–0.08%; and Fe and Mn less than 0.05%.

It should be noted that the Fe content of sample FJ-1–2 (FJ-1: 0.03–0.06; FJ-2: 0.04–0.06) is different from that of sample FJ-3–4 (FJ-3: ± 0.01 ; FJ-4: ± 0.01), while the content of other major elements is nearly identical. It is thought that the difference in Fe content is related to the metallogenic stage.

4.4.2. Micro Area X-ray Fluorescence Spectrum (Micro-XRF)

Micro-XRF analysis was performed on four Fujian calcite samples. A relatively flat surface on each sample has been chosen to analyse the distribution of Ca, O, Rb, Si, Sr, Mg, Al, Mn, Fe, and other elements. This study focuses on the element distribution of Ca, O, Mg, Mn, and Fe. Figure 5 depicts the element distribution of the four samples and an enlarged view of the selected micro area, and Table A2 displays the corresponding element concentrations.

Most of the major elements in the four samples, such as Ca, O, and Mg, were distributed uniformly in the micro area with no significant concentration differences. However, elements such as Fe and Mn are distinguishable from others. Fe and Mn were distributed relatively uniformly in the micro area of FJ-1 and FJ-2 samples, with concentrations of 0.06% and 0.05%, respectively. However, FJ-3 and FJ-4 samples exhibit noticeable depletion of Fe and Mn, with only a trace enrichment in the fractures, which is consistent with the XRF test results. The trace enrichment in calcite fractures may be related to the quartz, dolomite and other minerals that fill it [19].

The above analysis can prove that, in addition to CaCO₃, Fujian calcite samples also contain trace amounts of Fe, Mn, Mg, and other elements. Only Fe and Mg have certain content changes, but they are all evenly distributed.

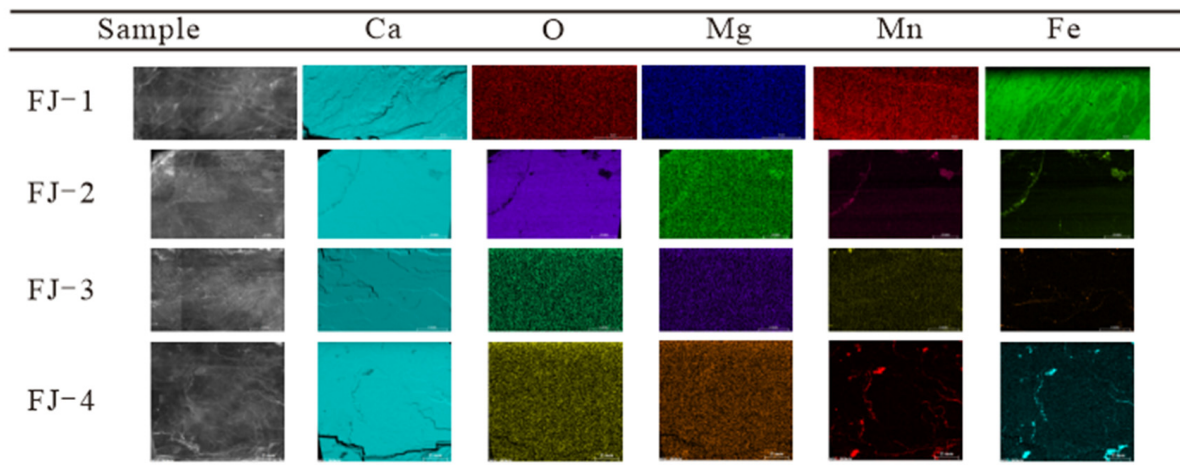


Figure 5. Morphologies and elements distribution of FJ-1, FJ-2, FJ-3, and FJ-4.

4.5. C-O Isotope Characteristics

C-O isotope test results of four calcite samples and a $\delta^{13}\text{C}$ - $\delta^{18}\text{O}$ diagram are shown in Table 2 and Figure 6. Oxygen isotopes are converted into SMOW (standard mean ocean water) by the equilibrium equation proposed by Friedman [20] et al.

$$\delta^{18}\text{O}_{\text{V-SMOW}} = 1.03086 \times \delta^{18}\text{O}_{\text{V-PDB}} + 30.86, \quad (1)$$

Table 2. C-O isotopic compositions (‰) of FJ-1, FJ-2, FJ-3, and FJ-4.

	$\delta^{13}\text{C}_{\text{V-PDB}}$ (‰)	$\delta^{18}\text{O}_{\text{V-PDB}}$ (‰)	$\delta^{18}\text{O}_{\text{V-smow}}$ (‰)
FJ-1	2.08	−16.98	13.36
FJ-2	2.22	−17.47	12.85
FJ-3	3.70	−14.24	16.18
FJ-4	3.61	−15.61	14.77

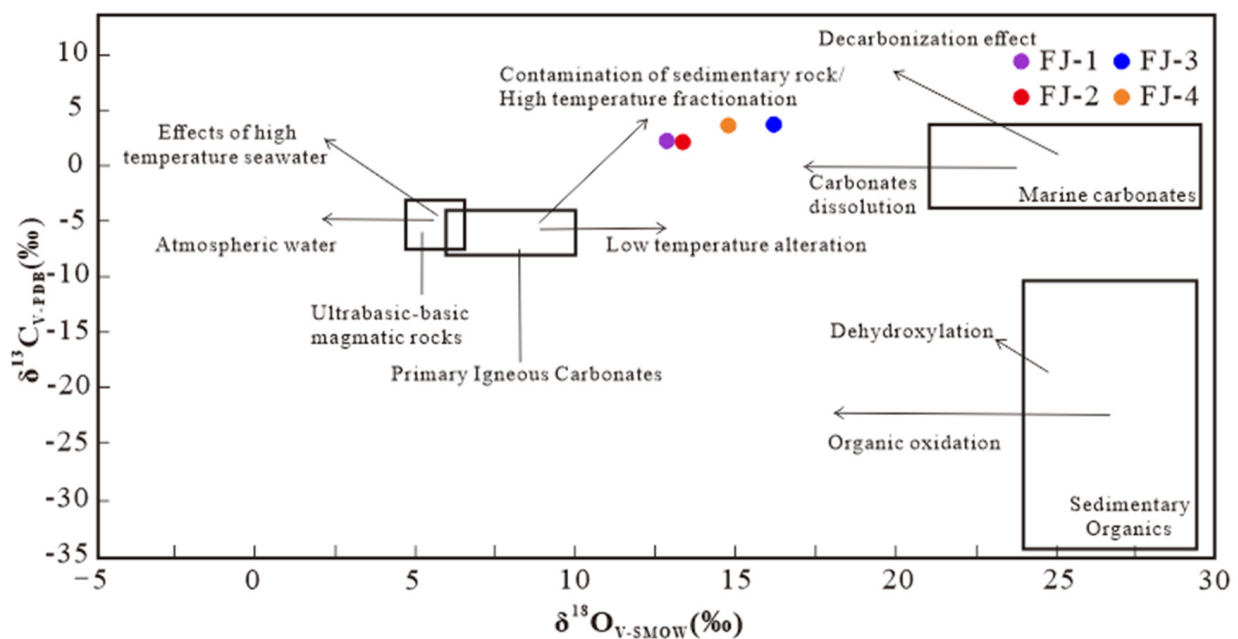


Figure 6. $\delta^{13}\text{C}$ - $\delta^{18}\text{O}$ diagram of Fujian calcite samples [21,22].

The $\delta^{13}\text{C}_{\text{V-PDB}}$ value ranges from 2.08‰ to 3.70‰, with an average of 2.90‰; and the $\delta^{18}\text{O}_{\text{V-SMOW}}$ value is between 12.85‰ and 16.18‰, with an average of 14.29‰. The projection points of the four samples are found to be roughly distributed in a small range between primary igneous carbonate and marine carbonates. It indicates that the C in Fujian calcites has a complex multi-source feature and has been altered or modified after sedimentation.

5. Discussion

5.1. Precipitation Mechanism of Fujian Calcites

Combining XRF and Micro-XRF results, it can be found that Fujian calcites contain a trace amount of Mn, Fe, Sr, and other impurity elements. We believed that these elements entered the calcite lattice by isomorphically replacing Ca^{2+} [23].

It is worth noting that the Fe and Mn content of FJ-1–2 is higher than that of FJ-3–4, so the four samples can be divided into two groups based on the Fe content (Figure 7). According to previous studies, the calcite in different metallogenic stages contains different Fe and Mn contents. The Fe and Mn contents are significantly higher in the metallogenic stage than in the non-metallogenic stage. The Fe content decreases rapidly from the metallogenic stage to the late-metallogenic stage [24]. Fe and Mn content decline may be related to the pre-crystallisation of Fe and Mn-rich skarn minerals [25]. The distribution of Fe-Mn content in calcite from Baoshan (BS), Huangshaping (HSP) polymetallic deposits, and the Oka mining area in Canada [26] are shown in Figure 7 (the larger the number, the later the stage), showing a noticeable decline trend from early- to late- metallogenic. Therefore, we believe that these four calcite samples formed in different stages: FJ-1–2 was formed in the metallogenic stage, while FJ-3–4 was formed in the late-metallogenic stage.

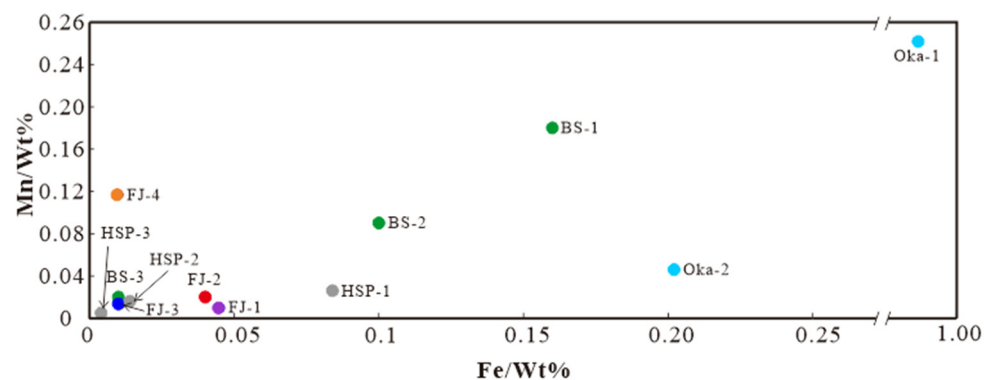


Figure 7. Fe-Mn diagram of Fujian calcite samples.

In recent years, the study of mineral isotopic characteristics has become the most powerful tool for studying the genesis of minerals and deposits [27–29]. The C-O isotopic composition of calcite is an effective method to explore its genesis. According to the $\delta^{13}\text{C}$ - $\delta^{18}\text{O}$ diagram of calcite samples, $\delta^{13}\text{C}_{\text{V-PDB}}$ values are located in a small range between mantle carbonatite and marine carbonate, indicating that the carbon may come from (1) primary igneous carbonatite that has been contaminated by sedimentary rocks or high-temperature fractionation; and (2) dissolution of marine carbonate [30]. Furthermore, the carbon isotopic composition of Fujian calcite is higher than that of sedimentary organic, ruling out the possibility that sedimentary organic provides C for calcite. The C-O isotopic composition of Fujian calcite suggests that its C may have complex multiple source characteristics.

The C-O isotopic composition of hydrothermal calcite is closely related to the C-O isotope composition of the ore-forming fluid, the mineral precipitation temperature, and the type of dissolved carbon in the hydrothermal fluid [25,31]. Calcite formation necessitates the presence of oxidized carbonaceous species in the fluid, such as $[\text{HCO}_3]$, CO_2 , and others. The C isotopic composition of Fujian calcite varies in a small range, with the projection point at the $\delta^{13}\text{C}$ - $\delta^{18}\text{O}$ diagram nearly horizontally distributed along the X axis. Previous studies suggest this phenomenon could be caused by: (1) CO_2 degassing, and (2) water-rock

reaction of fluid and surrounding rock [32,33]. The $\delta^{18}\text{O}_{\text{V-SMOW}}$ value of Fujian calcite varied more than the $\delta^{13}\text{C}_{\text{V-PDB}}$ value, indicating that the C in Fujian calcite is more likely to come from the dissolution of marine carbonate rocks. Since the mantle-derived fluid is clearly depleted of $\delta^{18}\text{O}$ compared with marine carbonate rocks, the $\delta^{18}\text{O}_{\text{V-SMOW}}$ value of Fujian calcite gradually increases from the early to the late-metallogenic stage, which reasonably reflects that $\delta^{18}\text{O}$ depleted mantle-derived fluid occurred in water-rock reaction with a surrounding rock during migration and mineralization. Therefore, the ore-forming fluid gradually enriched $\delta^{18}\text{O}$, causing calcite to enrich $\delta^{18}\text{O}$.

In conclusion, the formation process of Fujian calcite may be as follows: the initial ore-forming fluid derived from the mantle migrated upward along deep faults. During this process, the dissolution of marine carbonate or contamination of sedimentary rocks occurred, and the large-scale fluid migration occurred during the mineralization process. Calcite gradually precipitates from the fluid after a complete water-rock reaction between the fluid and the surrounding rock [34,35].

5.2. Origin Characteristics of Fujian Calcite

Mineralogical characteristics: The calcite samples from Fujian are colourless or yellow brown, with high transparency and regular crystal morphology. The magnification observation reveals two sets of surface cleavage and no significant internal inclusions.

Spectral characteristics: It can be seen from Figure 2 that Fujian calcites have relatively standard infrared spectrum results. They all have 709 cm^{-1} , 887 cm^{-1} , and 1480 cm^{-1} characteristic absorption peaks in the fingerprint region. Figure 3 shows that the Raman spectrum of Fujian calcite is the same as the RRUFF standard spectrum and has the same characteristic absorption peak. Therefore, Fujian calcite is pure calcite and has uniform spectroscopic characteristics.

Phase composition: Fujian calcite's diffraction patterns match with the RRUFF standard patterns of calcite, indicating that the mineral compositions of Fujian calcite are pure calcite, without impurities minerals [36].

Major elements composition: Fujian calcite is primarily composed of Ca and contains trace amounts of Mn, Fe, Si, Sr, and other elements. The content of most of major elements is similar across samples and the distribution is uniform.

C-O isotope characteristics: The $\delta^{13}\text{C}_{\text{V-PDB}}$ value ranges from 2.08‰ to 3.70‰, with an average of 2.90‰; the $\delta^{18}\text{O}_{\text{V-SMOW}}$ value is between 12.85‰ and 16.18‰, with an average of 14.29‰. The C-O isotopic composition of Fujian calcite is similar, with little variation, indicating that it is relatively uniform.

In conclusion, Fujian calcite is pure with CaCO_3 as the main component, trace Fe, Mn, and other impurities elements and no other minerals in its phase composition. Furthermore, its spectral, major element, and C-O isotope characteristics are highly concordant. Therefore, Fujian calcite is a novel calcite with the potential to be used as stand samples.

6. Conclusions

We have investigated the phase composition, spectral and geochemistry characteristics of calcite crystals from Fujian, China, through Fourier infrared and Raman spectroscopy, XRF, and Micro-XRF. These results are used to report the systematic mineralogical characteristics of the calcite from Fujian, China and to discuss its possible genesis. In this paper, the analysis and summary of all samples provide characteristics of a new production area of calcite not found in the RRUFF database. According to C-O isotope analysis, during the formation process of Fujian calcite, the dissolution of marine carbonate or contamination of sedimentary rocks may occur. Calcite gradually precipitates from the fluid after a complete water-rock reaction. We think Fujian calcite is very pure calcite and has the potential to be used as stand samples.

Author Contributions: Writing and experimental data processing, Z.-Y.Z. and Y.-T.L.; writing-review and editing, B.X. and Y.Z.; methodology, B.X. and Y.Z. All authors have read and agreed to the published version of the manuscript.

Funding: This research was funded by the National Key Technologies R&D Program (2019YFA0708602 2020YFA0714800) and the National Natural Science Foundation of China (42222304, 42073038, 41803045, 42202084), Young Talent Support Project of CAST, the Fundamental Research Funds for the Central Universities (Grant no. 265QZ2021012), and IGCP-662.

Data Availability Statement: The data presented in this study are available within this article.

Acknowledgments: We thank the editor and reviewers for their constructive comments which helped in improving our paper. This is the 11th contribution of B.X. for the National Mineral Rock and Fossil Specimens Resource Center.

Conflicts of Interest: The authors declare no conflict of interest.

Appendix A

Table A1. Chemical compositions of analyzed calcite from Fujian analyzed by XRF (in wt.%).

		CaO/%	SiO ₂ /%	K ₂ O/%	Fe ₂ O ₃ /%	MnO/%	CuO/%	Br/%	SrO/%
FJ-1	1	98.64	0.79	0.08	0.06	0.01	0.01	/	/
	2	93.28	0.68	0.07	/	/	0.01	/	0.03
	3	98.87	0.69	/	0.03	0.01	/	0.01	0.05
	4	98.53	0.76	0.07	0.05	0.01	/	0.01	0.06
	5	94.83	0.63	0.07	0.04	/	/	/	0.04
FJ-2	1	98.97	0.68	0.07	0.06	0.02	0.01	/	0.02
	2	99.06	0.71	0.06	0.06	0.01	0.01	/	0.04
	3	92.55	0.71	0.09	/	0.02	0.01	0.01	0.03
	4	99.08	0.66	0.08	/	0.02	0.01	0.01	0.03
	5	98.80	0.70	0.07	0.04	0.02	/	0.01	0.03
FJ-3	1	91.25	0.66	/	/	0.01	/	0.01	0.06
	2	98.86	0.67	/	0.01	0.02	0.01	/	0.06
	3	93.19	0.64	/	/	0.01	/	0.01	0.04
	4	98.61	0.75	0.06	/	0.01	/	0.01	0.05
	5	98.70	0.67	0.07	0.01	0.018	0.01	/	0.06
FJ-4	1	93.55	0.65	/	/	0.126	/	/	0.10
	2	92.17	0.65	0.07	/	0.092	/	/	0.09
	3	91.94	0.67	0.07	/	0.093	/	0.01	0.10
	4	97.83	0.19	0.07	0.01	0.154	0.02	/	0.14
	5	98.67	0.70	/	0.01	0.119	/	0.01	0.12

Table A2. Chemical compositions of analyzed calcite from Fujian analyzed by Micro-XRF (in wt.%).

	FJ-1	FJ-2	FJ-3	FJ-4
Ca	39.52	39.53	39.56	39.60
C	11.93	11.94	11.92	11.98
O	47.69	47.73	47.98	47.89
Mg	0.14	0.18	0.16	0.19
Mn	0.01	0.01	0.01	0.01
Fe	0.08	0.05	0.02	0.01

References

1. Zhou, J.-X.; Huang, Z.-L.; Zhou, G.-F.; Zeng, Q.-S.C. O Isotope and REE Geochemistry of the Hydrothermal Calcites from the Tianqiao Pb-Zn Ore Deposit in NW Guizhou Province, China. *Geotecton. Metallog.* **2012**, *36*, 93–101.
2. Huang, Z.-L.; Li, X.-B.; Zhou, M.; Li, W.-B.; Jin, Z.-G. REE and C-O Isotopic Geochemistry of Calcites from the World-class Huize Pb-Zn Deposits, Yunnan, China: Implications for the Ore Genesis. *Acta Geol. Sin.* **2010**, *84*, 597–613. [[CrossRef](#)]
3. Hou, Z.-Q.; Tian, S.-H.; Xie, Y.-L.; Yuan, Z.-X.; Yang, Z.-S.; Yin, S.-P.; Fei, H.-C.; Zou, T.-R.; Li, X.-Y.; Yang, Z.-M. Mianning-Dechang Himalayan REE belt associated with carbonatite-alkalic complex in eastern Indo-Asian collision zonesouthwest China: Geological characteristics of REE deposits and a possible metallogenic model. *Miner. Depos.* **2008**, *2*, 145–176.

4. Hou, Z.-Q.; Liu, Y.; Tian, S.-H.; Yang, Z.-M.; Xie, Y.-L. Formation of carbonatite-related giant rare-earth-element deposits by the recycling of marine sediments. *Sci. Rep.* **2015**, *5*, 10231. [CrossRef] [PubMed]
5. Tang, B.-L.; Liu, Y.-C.; Yue, L.-L.; Ma, W.; Zhuang, L.-L. Hydrothermal fluid evolution in Huachangshan Pb-Zn deposit in Yunnan: the evidences of calcite REE and C-O isotope analyses. *Acta Geol. Sin.* **2022**. [CrossRef]
6. Tang, Y.-Y.; Bi, X.-W.; He, L.-P.; Wu, L.-Y.; Feng, C.-X.; Zou, Z.-C.; Tao, Y.; Hu, R.-Z. Geochemical characteristics of trace elements fluid inclusions and carbon-oxygen isotopes of calcites in the Jinding Zn-Pb deposit, Lanping, China. *Acta Petrol. Sin.* **2011**, *27*, 2635–2645.
7. Tang, G.-Q.; Li, X.-H.; Li, Q.; Liu, Y.; Ling, X.X. A new Chinese national reference material (GBW04481) for calcite oxygen and carbon isotopic microanalysis. *Surf. Interface Anal. SIA* **2020**, *52*, 190–196. [CrossRef]
8. Hu, A.-X.; Wen, J.; Peng, J.-T. Rare earth elements' geochemistry of calcites in the Xikuangshan antimony deposit, central Hunan and its indicative significance for prospecting. *Acta Mineral. Sin.* **2023**, *43*, 38–48. [CrossRef]
9. Wang, H.; Zhong, F.-J.; Wu, D.-H.; Pan, J.-Y.; Shu, T.-T.; Yan, J.; Li, D.-H.; Zhang, R.; Liu, B. Characteristics and Geological Implications of Carbon and Oxygen Isotopes and REE of Calcite from Egongtang Deposit in Northern Guangdong Province. *Chin. Rare Earths* **2022**. [CrossRef]
10. Xing, Z.-J.; Leon, B.; Zhonghua, H.; Wengang, L. Sm-Nd isochron age and Sr-Nd isotopes of the calcite from the Nibao gold deposit in the Youjiang Basin, SW China. *Resour. Geol.* **2022**, *72*, e12292.
11. Myint, A.Z.; Wagner, T.; Fusswinkel, T. Calcite trace element geochemistry of Au deposits in the Singu-Tabekkyin Gold District, Myanmar: Implications for the sources of ore-forming fluids. *Ore Geol. Rev.* **2022**, *145*, 104692. [CrossRef]
12. RRUFF Database. Available online: <https://rruff.info/calcite/display=default/R040070> (accessed on 1 October 2022).
13. Xu, B.; Hou, Z.Q.; Griffin, W.L.; Lu, Y.; Belousova, E.; Xu, J.F.; O'Reilly, S.Y. Recycled volatiles determine fertility of porphyry deposits in collisional settings. *Am. Mineral.* **2021**, *106*, 656–661. [CrossRef]
14. Xu, B.; Kou, G.; Etschmann, B.; Liu, D.; Brugger, J. Spectroscopic, Raman, EMPA, Micro-XRF and Micro-XANES Analyses of Sulphur Concentration and Oxidation State of Natural Apatite Crystals. *Crystals* **2020**, *10*, 1032. [CrossRef]
15. Xu, B.; Hou, Z.-Q.; Griffin, W.L.; O'Reilly, S.Y.; Zheng, Y.C.; Wang, T.; Xu, J.F. In-situ mineralogical interpretation of the mantle geophysical signature of the Gangdese Cu-porphyry mineral system. *Gondwana Res.* **2022**, *111*, 53–63. [CrossRef]
16. Yang, N.; Kuang, S.-Y.; Yue, Y.-H. Infrared Spectra Analysis of Several Common Anhydrous carbonate Minerals. *Mineral. Petrol.* **2015**, *35*, 37–42. [CrossRef]
17. Zhu, Y.; Li, Y.-Z.; Lu, A.-H.; Ding, H.-D.; Li, Y.; Wang, C.-Q. Middle and far infrared spectroscopic analysis of calcite, dolomite and magnesite. *Earth Sci. Front.* **2022**, *29*, 459–469. [CrossRef]
18. He, J.-L.; Pan, Z.-X.; Ran, J. The Application of Laser Raman Spectroscopy to Rock and Mineral Identification. *Acta Geol. Sichuan* **2016**, *36*, 346–349.
19. Hu, Z.-Z.; Yan, X.; Du, G.; Wang, G.; Xu, G.-D.; He, J.-L.; Jin, L.; Lan, M.-G.; He, X.-H. The Calcite 811N, a potential isotope standard material for isotopic analyses of carbon, oxygen and strontium. *Sediment. Geol. Tethyan Geol.* **2022**, *15*, 1–24. [CrossRef]
20. Friedman, I.; O'Neil, J.R. Compilation of stable isotope fractionation factors of geochemical interest. *Data Geochem.* **1977**, *440*, 1–55.
21. Liu, J.-K.; Deng, M.-G.; Mao, L.-Z.; Wang, D.; Geng, Q.-W. Characteristics and Indication of Carbon-Oxygen Isotopes and Rare Earth Elements of Hydrothermal Calcite from the Mengxing Pb-Zn Deposit, Western Yunnan. *Geol. Explor.* **2021**, *57*, 852–864.
22. Tian, S.-H.; Hou, Z.-Q.; Yang, Z.-S.; Chen, W.; Yang, Z.-M.; Yuan, Z.-X.; Xie, Y.-L.; Fei, H.-C.; Yin, S.-P.; Liu, Y.-C.; et al. Geochronology of REE deposits in Mianning-Dechang REE metallogenic belt: Constraints on duration of hydrothermal activities and tectonic mode for carbonatite-alkalic complexes in southwestern Sichuan. *Miner. Depos.* **2008**, *27*, 177–187.
23. Zhu, Z.-M.; Zheng, R.-C.; Luo, L.-P.; Zhou, J.-Y.; Shen, B.; Chen, J.-B. Element Geochemistry and its genetic significant of calcite in the MuLuo REE deposit, SiChuan province. *Acta Mineral. Sin.* **2008**, *28*, 455–460.
24. Wang, J.-S.; Han, Z.-C.; Li, C.; Gao, Z.-H.; Yang, Y.; Zhou, G.-C. REE, Fe and Mn Contents of Calcites and Their Prospecting Significance for the Banqi Carlin-type Gold Deposit in Southwestern China. *Geotecton. Metallog.* **2018**, *42*, 494–504.
25. Zheng, Y.-F. Theoretical modeling of stable isotope systems and its applications to geochemistry of hydrothermal ore deposits. *Miner. Depos.* **2021**, *20*, 69–76.
26. Chen, Q.; Gao, X.; Tan, S.; Huang, J. Geochemical characteristics and indicative significance of hydrothermal vein in the Xiangyangping uranium ore deposit, middle segment of Miao'er Mountain, northern Guangxi. *Acta Petrol. Mineral.* **2020**, *39*, 795–807.
27. Xu, B.; Hou, Z.Q.; Griffin, W.L.; Zheng, Y.C.; Wang, T.; Guo, Z.; Hou, J.; Santosh, M.; O'Reilly, S.Y. Cenozoic lithospheric architecture and metallogenesis in Southeastern Tibet. *Earth-Sci. Rev.* **2021**, *214*, 103472. [CrossRef]
28. Xu, B.; Griffin, W.L.; Xiong, Q.; Hou, Z.Q.; O'Reilly, S.Y.; Guo, Z.; Pearson, N.; Greau, Y.; Zheng, Y.C. Ultrapotassic rocks and xenoliths from South Tibet: Contrasting styles of interaction between lithospheric mantle and asthenosphere during continental collision. *Geology* **2017**, *45*, 51–54. [CrossRef]
29. Xu, B.; Hou, Z.Q.; Griffin, W.L.; O'Reilly, S.Y. Apatite halogens and Sr–O and zircon Hf–O isotopes: Recycled volatiles in Jurassic porphyry ore systems in southern Tibet. *Chem. Geol.* **2022**, *605*, 120924. [CrossRef]
30. Yang, C.-F.; Gu, X.-X.; Liu, J.-Z.; Wang, Z.-P.; Chen, F.-E.; Wang, D.-F.; Chen, L.-Y.; Li, J.-H. Rare Earth Elements and C-O-Sr Isotopic Geochemical Characteristic of Hydrothermal Calcites of the Carlin-Type Gold Deposits in the Huijiabao Orefield, Southwestern Guizhou, China. *Bull. Mineral. Petrol. Geochem.* **2021**, *40*, 124–137. [CrossRef]
31. Zheng, Y.-F.; Hoefs, J. Carbon and oxygen isotopic covariations in hydrothermal calcites. *Miner. Depos.* **1993**, *28*, 79–89. [CrossRef]

32. Spangenberg, J.; Fontboté, L.; Sharp, Z.D.; Hunziker, J. Carbon and oxygen isotope study of hydrothermal carbonates in the zinc-lead deposits of the San Vicente district, central Peru: A quantitative modeling on mixing processes and CO₂ degassing. *Chem. Geol.* **1996**, *133*, 289–315. [[CrossRef](#)]
33. Wu, L.-Y.; Hu, R.-Z.; Peng, J.-T.; Bi, X.-W.; Chen, H.-W.; Wang, Q.-Y.; Liu, Y.-Y. Carbon and oxygen isotopic compositions of Chaishan Pb-Zn deposit in the Shizhuyuan ore field and implications. *Geochimica* **2009**, *38*, 242–250. [[CrossRef](#)]
34. Li, R.-Q. Variation of Mg-Fe-Mn contents of calcite and its significance in Southern Hunan polymetallic province. *Hunan Geol.* **1995**, *14*, 99–105.
35. Shuang, Y.; Bi, X.-W.; Hu, R.-Z.; Peng, J.-T.; Li, Z.-L.; Li, X.-M.; Yuan, S.-D.; Qi, Y.-Q. Re-e Geochemistry Of Hydrothermal Calcite From Tin-Polymetallic Deposit And Its Indication Of Source Of Hydrothermal Ore-Forming Fluid. *J. Mineral. Petrol.* **2006**, *26*, 57–65.
36. Crowley, S.F. Mineralogical and chemical composition of international carbon and oxygen isotope calibration material NBS19, and reference materials NBS18, IAEA-CO-1 and IAEA-CO-8. *Geostand. Geoanalytical Res.* **2010**, *34*, 193–206. [[CrossRef](#)]

Disclaimer/Publisher's Note: The statements, opinions and data contained in all publications are solely those of the individual author(s) and contributor(s) and not of MDPI and/or the editor(s). MDPI and/or the editor(s) disclaim responsibility for any injury to people or property resulting from any ideas, methods, instructions or products referred to in the content.